J Mater Sci (2010) 45:2106–2111
DOI 10.1007/s10853-009-4147-7

HTC2009

A novel approach to determine high temperature wettability and interfacial reactions in liquid metal/solid interface

Sascha Frenznick · Srinivasan Swaminathan · Martin Stratmann · Michael Rohwerder

Received: 31 May 2009 / Accepted: 18 December 2009 / Published online: 8 January 2010

Abstract In many technical processes, high temperature wetting of a liquid metal phase on a solid substrate occurs via an extensive chemical reaction and the formation of a new solid compound at the interface. For instance, good adhesion of the zinc coating to the steel surface is one of the most important requirements that the hot-dip galvanizing process has to fulfill. Good adhesion directly depends on the formation of a defect-free Fe_2Al_5 inhibition layer at the interface. The complex surface chemistry of oxides on the steel surface which is a result of segregation and selective oxidation upon recrystallization annealing significantly influences the kinetics of the correlated reactive wetting. This article presents the development of a novel advanced technique for the investigation of high temperature wetting process up to a temperature of 1100 K and provides first new insights in the mechanisms of the reactive wetting process in presence of oxides on the surface. The method is based on the sessile drop method with an additional spinning technique to get rid off the liquid metal phase at any chosen wetting time, thusly opening the way to access the interfacial reaction layer directly. The presented work focuses on model alloys of interest which are mainly relevant to the industrial steel grades. Emphasis is put both on the wettability of liquid Zn and on the interfacial reactions during reactive wetting process. Insights into such reactive phenomena are fundamental demand to improve the hot-dip galvanizability of advanced high strength steel grades.

S. Frenznick · S. Swaminathan (✉) · M. Stratmann · M. Rohwerder
Max-Planck-Institut für Eisenforschung GmbH, Max-Planck Str. 1, 40237 Düsseldorf, Germany
e-mail: s.swaminathan@mpie.de

Introduction

High temperature wettability and their corresponding interfacial reactions play a crucial role in many technical processes, from soldering in microelectronics and production of metal/ceramic composites, to hot-dip galvanizing in mass production of zinc-coated steel sheet [1–5]. In all these processes, it is important that the interfacial reactions should proceed fast enough to ensure good wetting within the allotted time window. For instance, in hot-dip galvanizing, the steel sheet moves at high speed through a zinc bath (about 2–3 s immersion time) and real-time monitoring of the interfacial reaction is absolutely not feasible. Most of the currently applied hot-dip galvanizing simulation techniques rely solely on monitoring the spreading of the liquid zinc phase on the substrate. Information on the interfacial reaction layer at the buried interface cannot be directly obtained. The reaction layer has to be laid open by chemical or by electrochemical removal of the solidified former liquid phase. This is not only a very tedious procedure, but also usually not perfect, i.e., an effect on the interfacial reaction cannot be completely avoided. Furthermore, very often the kinetics observed during typical simulation routines are not the same as in the actual technical process, due to insufficient atmospheric control. Hence, a dedicated experimental setup was developed which not only allows to operate in a parameter window (e.g., at dew point of less than 193 K), but also to obtain information about the fundamental mechanisms of the wetting process during hot-dip galvanizing [6–8].

Basically, high-strength steels for automotive industry undergo recrystallization annealing before hot-dip galvanizing. The problem here is, although the annealing is being done in a reducing atmosphere (N_2–5%H_2), segregation and

selective surface oxidation of the minor alloying elements make the steel surface unsuitable for subsequent galvanizing. A number of studies reported that zinc wettability rapidly decreases with the occurrence of external selective oxidation of less noble elements, i.e., Al, Si, and Mn oxides covering the surface of the steel [9, 10]. Earlier investigations have shown that transition from external to less harmful internal oxidation is achievable by choosing appropriate dew point in the annealing atmosphere [7, 11]. Moreover, the quality of the Zn coating strongly depends on the formation of an undistorted Fe_2Al_5 inhibition layer at the interface [12–14]. The reaction occurring at the steel/liquid zinc interface has been modeled by many researchers in order to understand the galvanizing kinetics [15, 16]. Webb et al. [17] reported that the progress in molecular dynamic (MD) simulation is capable of investigating reactive wetting in realistic metal systems exhibiting significantly different chemistry. Avraham and Kaplan [18] pointed out that the interface reaction at the solid-liquid interface governs the spreading kinetics of the liquid metal, for example, spreading of the Al drop on TiO_2 is governed by the reduction of TiO_2 and the formation of Al_2O_3 at the interface. Protsenko et al. [19] explained the role of intermetallic formation in wetting of clean and oxidized Fe by liquid metals. For a surface covered by thin oxide films, the wetting is strongly improved by intermetallic formation reactions leading to replacement of the oxidized surface by a clean surface of an intermetallic compound. Here the question in hot-dip galvanizing is how the oxide, i.e., the nature of oxide (surface chemistry), the overall oxide coverage, the island size, and the distribution of the oxides, affects the wettability and the interfacial reaction. For this purpose a novel experimental setup Hot Melt Rotator (HoMeR, also denoted as the liquid zinc spin coater) was designed at Max-Planck-Institut für Eisenforschung (MPIE), which comprises thermal treatment and galvanizing units [7, 8]. This unique feature allows spinning off the liquid Zn (with 0.23% Al and <0.005% Fe) from the substrate after visualizing the wetting behavior (i.e., sessile drop contact angle measurement) with high rotation speed in order to obtain the newly formed interface without any further physical/chemical treatments. This combination of contact angle detection and interfacial accessibility provides an excellent method to gain a fundamental understanding of the reactions taking place during the galvanizing process. The aim of the present investigation is to show how the Si, Mn oxides and their surface coverage influence the wetting kinetics. It was found in this work that oxide islands can be overgrown by the Fe_2Al_5 reaction layer. Specifically this work identifies that the overall wetting kinetics is completely governed by this overgrowing of the oxide islands.

Experimental

Model alloys and specimen preparation

Binary model alloys of Fe–Si and Fe–Mn (with different compositions of Si and Mn) were prepared and hot rolled at MPIE. The bulk compositions of Si in the Fe–Si and of Mn in the Fe–Mn alloys are presented in Table 1. The specimens (of size 15 mm × 15 mm) were ground with SiC paper (up to grit 4000) and rinsed with ethanol, finally they were polished with diamond paste (first 3 μm followed by 1 μm) to a mirror finish. After polishing the specimens were cleaned ultrasonically in ethanol for 10 min.

Annealing and wetting

The reduction annealing and subsequent zinc wetting experiments were carried out in an 'in-house' built hot melt rotator (HoMeR, also denoted as the liquid zinc spin coater). The details of the experimental setup are described elsewhere [6–8]. The specimens were annealed (in the reaction chamber of the HoMeR) at 820 °C for 1 min in N_2–5%H_2 gas atmospheres with dew point of −30 °C. This is an industrially relevant short-term annealing condition. The dew point of the annealing atmosphere is controlled by a portable gas mixing system with oxalic acid columns for establishing the humidity as well as with humidity and oxygen sensors.

To simulate the galvanizing condition, the specimen annealed at a specified dew point in the reaction chamber is heated to 470 °C in the main chamber of the HoMeR where the Zn-syringe is installed. In order to avoid the oxidation of zinc, very low dew point (≤−80 °C) is maintained at the main chamber. A zinc drop is placed on the specimen and the wetting behavior is monitored by the video system. The contact angle is measured by a custom-made analysis program. After a given time the spin coater starts with a rotation speed up to 3500 rpm. Therefore, the spin coater is able to simulate reaction layers with a very short reaction time. During the fast spinning process nearly all residual liquid zinc is driven off the surface and opens the way to directly access the interface. Since the HoMeR is UHV compatible system, direct transfer of specimen (without air exposure) to the surface analysis tools such as scanning electron microscopy (SEM) and X-ray photoelectron spectroscopy (XPS) is realized. It is important to notice

Table 1 Composition of the model alloys investigated

Binary model alloys	Compositions (wt%)
Fe–Si	Fe–0.25Si, Fe–1.0Si, Fe–1.5Si, Fe–3.0Si
Fe–Mn	Fe–0.5Mn, Fe–1.0Mn, Fe–3.0Mn

that the specimen surface chemistry as obtained during heat treatment in the reaction chamber is not changed significantly upon re-heating prior to zinc coating.

Results and discussion

In this study, the compositions of Si and Mn model alloys have been chosen in accordance with the newly developing steel grades. Surface chemistry of the oxides and their coverage play vital role in hot-dip galvanizing process. Basically, these factors can be controlled by the process parameters, such as dew point of the annealing atmosphere. Figure 1a shows the surface morphology of the Fe–0.25Si alloy after annealing at dew point −30 °C, showing very tiny Si oxides decorating not only the grain boundaries but also the grains. It is important to note that this annealing condition is reducing for Fe and only oxidation of Si occurs. According to the Cassie equation [20], the zinc wetting is predominantly determined by the relative composition (i.e., surface coverage) of the oxide and metal phase,

$$\cos\theta = a_{\text{oxide}}\cos\theta_{\text{oxide}} + (1 - a_{\text{oxide}})\cos\theta_{\text{metal}} \quad (1)$$

where a_{oxide} is the surface coverage of the oxide, θ_{oxide} and θ_{metal} are the contact angle in equilibrium state of the oxide and metal, respectively.

As the reactive wetting in the hot-dip galvanizing process depends on the growth of stable Fe-Al interfacial layer, the modified Avrami growth law [21] has been applied to the above Eq. 1, which leads to the new description of the dynamic Cassie equation as follows:

$$\cos\theta = \cos\theta_{\text{oxide}}\ a\ \exp(-kt^n) + \cos\theta_{\text{metal}}\ [1 - a\ \exp(-kt^n)] \quad (2)$$

where a is the initial surface coverage of the oxide, k is the Avrami constant (basically defines the kinetics), and n is the Avrami exponent.

This new dynamic Cassie equation has been applied to fit the experimental wetting curve to understand the kinetics of reactive wetting in the hot-dip galvanizing process. The measured contact angles of zinc on pure Fe are 5°, on SiO_2 150°, and on MnO 140°. Figure 1b shows the change of $\cos\theta$ with time during wetting of the zinc drop on Fe-0.25Si alloy annealed at dew point −30 °C. Within the first 2 s the contact angle decreases from 100° to about 70°, i.e., changes from the non-wetting to the wetting regime. In order to understand the wetting kinetics, the $\cos\theta$ versus t plot has been fitted by modified Avrami growth kinetics with Avrami exponent $n = 0.5$, which basically holds for the one-dimensional growth law. In this case, the fit provides a value for the initial oxide coverage of about 69% ($a = 0.69$) which seems to be reasonable in view of the high coverage of the surface by tiny oxide islands. By increasing the dew point of the annealing atmosphere, external surface oxidation can be decreased. Basically, the increase of the dew point, which in turn leads to an increase of surface oxygen content in the annealing atmosphere, leads to a higher inward oxygen permeability. It is quite obvious that oxygen diffuses deeper during annealing at high dew point since the oxygen-free surface adsorption rate is directly related to the partial pressure of oxygen in the annealing atmosphere. Figure 2a shows the surface morphology of Fe–0.25Si alloy annealed at an increased dew point of 0 °C, which clearly indicates the presence of less external oxidation. This is an excellent agreement with the observed fast wetting kinetics, as shown in Fig. 2b.

Similarly, investigations on various Fe–Si and Fe–Mn model alloys were carried out and their wetting kinetics have been compared by applying the modified Avrami

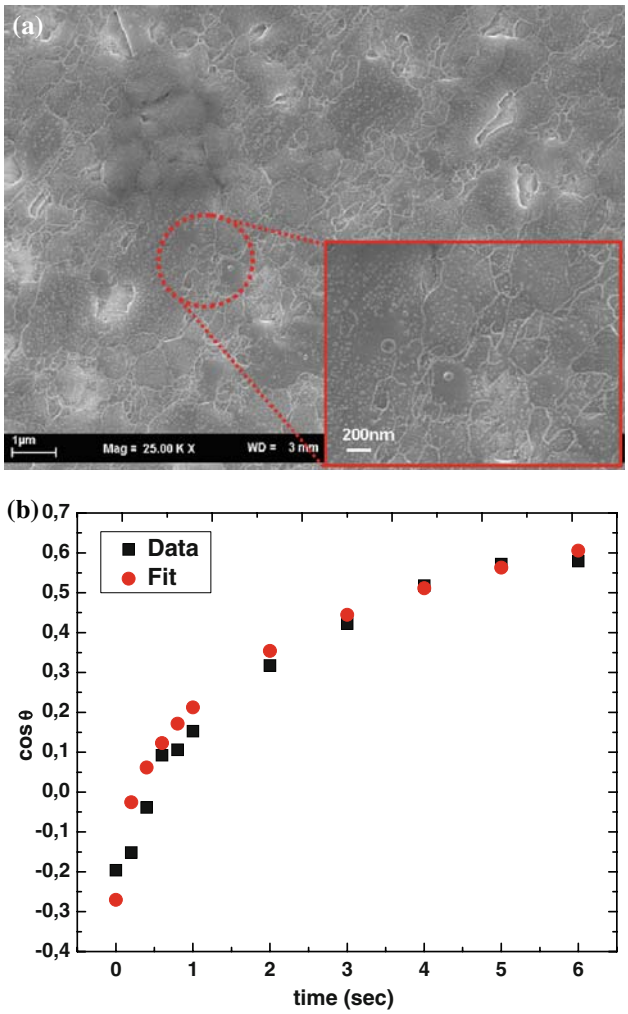

Fig. 1 **a** SEM image of the oxide coverage on a Fe–0.25Si alloy specimen annealed at a dew point of −30 °C, the *inset* figure shows a magnified image of the oxide islands, **b** cosine of the contact angle over time (wetting curve)

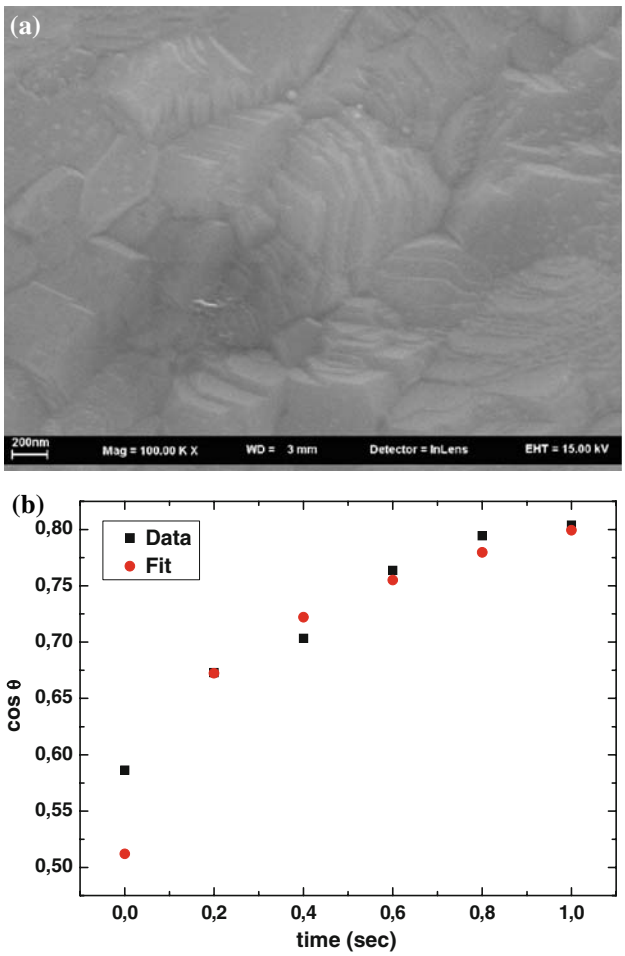

Fig. 2 **a** Surface morphology of a Fe–0.25Si alloy specimen annealed at high dew point (0 °C), **b** cosine of the contact angle over time (wetting curve)

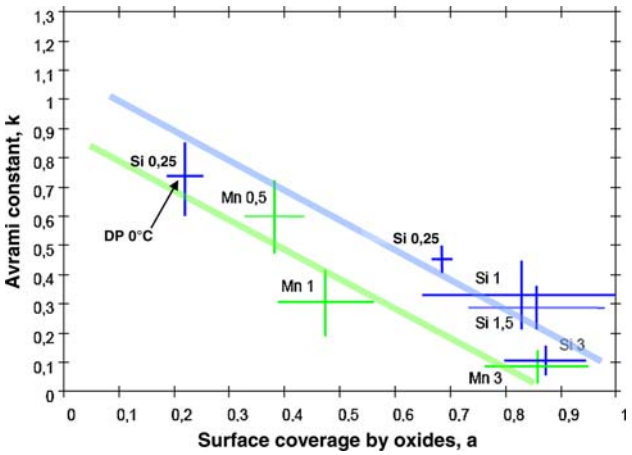

Fig. 3 The reactive wetting kinetics of various Fe–Si and Fe–Mn model alloys (annealed at DP −30 °C according to the procedure described in the experimental section, if not stated otherwise) described by plotting the kinetic constant '*k*' versus the oxide coverage '*a*', as obtained by introducing a modified Avrami growth law into the Cassie equation

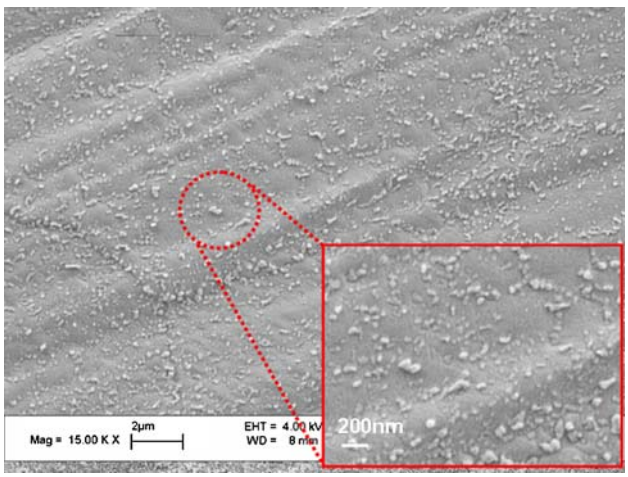

Fig. 4 SEM image of the oxide coverage on a Fe–1Mn alloy specimen annealed at dew point −30 °C, the *inset* figure shows a magnified image of the oxide islands

growth kinetics. Figure 3 correlates the kinetics of the reactive wetting with the initial oxide coverage of the different samples. Here as a measure for the wetting kinetics the Avrami factor '*k*' is taken, which is determined by the interfacial wetting kinetics as well as by geometric factors. This becomes directly obvious when comparing the '*k*' values obtained with the Fe–Si alloys with the ones obtained with the Fe–Mn alloys. For Fe–Mn alloys, at similar oxide coverage '*a*', the '*k*' values are smaller than the ones for the Fe–Si alloys. In fact, in spite of a much higher surface coverage with oxides (69%) for the case of the Fe–0.25Si alloy, the kinetic factor is higher than that of the Fe–1Mn alloy with an initial oxide coverage of about 47% (according to the fitting). This means that although the Fe–0.25Si alloy shows higher contact angle ($\theta > 90°$, i.e., non-wetting regime) in the beginning, the wetting kinetics is faster than on the Fe–1Mn alloy, in other words the surface coverage with the interfacial reaction layer Fe_2Al_5 grows much faster in the former case than in the latter one.

The reason becomes directly obvious on the basis of the surface morphology of both the alloys (Figs. 1a, 4), moreover, the thickness of the oxide islands formed on the Fe–0.25Si alloy is ∼10 nm, which is much lower than the thickness of the Mn–oxide islands (∼40 nm) formed on the Fe–1Mn alloy. On the surface of Fe–1Mn alloy annealed at dew point −30°C, the formed oxide islands are relatively larger in size (Fig. 4) in comparison to the ones observed on the Fe–0.25Si alloy; hence, the smaller size of the latter ones seems to lead to faster kinetics. The reason for that most likely is due to the fact that the growing Fe_2Al_5 crystals can overgrow small oxide islands more

Table 2 Oxide coverage of various Fe–Mn and Fe–Si binary model alloys

Model alloys	Surface coverage by oxides	
	Estimated from the fit (Avrami exponent, $n = 0.5$)	Estimated from the XPS analysis
Fe–Mn		
Fe–0.5Mn	0.38	0.34
Fe–1.0Mn	0.47	0.63
Fe–3.0Mn	0.85	0.78
Fe–Si		
Fe–0.25Si	0.69	0.56
Fe–1.0Si	0.83	0.51
Fe–1.5Si	0.86	0.57
Fe–3.0Si	0.87	0.87

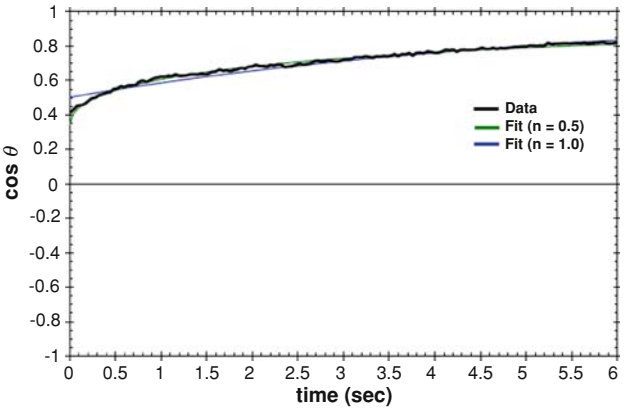

Fig. 5 The wetting curve (cosine of the contact angle over time) of a Fe–0.5Mn alloy specimen fitted by applying modified Avrami growth kinetics with Avrami exponent $n = 0.5$ and $n = 1$, respectively

easily than larger ones. This also means that on surfaces with small oxide islands more homogenous interfacial reaction layers should form. In the case of large oxide islands, the diffusion of Fe from the alloy substrate to the reaction front has to go all the way over the large oxide islands; hence, it is very difficult to form a closed inhibition layer. Obviously this might be the reason for the observation of the lower wetting kinetics on the Fe–Mn alloys, in spite of its relatively lower oxide coverage in comparison to the Fe–Si alloy. In order to compare the surface oxide coverage '*a*' as obtained from the fits of the measured contact angle curves with the Avrami-modified Cassie equation with measured values for '*a*', we estimated the oxide coverage of the samples prior to the wetting experiments, i.e., after the according annealing, by XPS analysis. The according oxide coverage values are listed in Table 2. The results listed in this table clearly show that the computed values (obtained for the Avrami exponent $n = 0.5$) agree well with the XPS analysis, i.e., the deviations are small. Just for the Fe–1Si and Fe–1.5Si alloys the values obtained from the fits deviate somewhat from the ones obtained by XPS. This is thought to be due to the complex oxide structure (oxide islands and iron spangled with tiny oxide islands). In order to check which Avrami exponent gives the best result, the wetting curves (cosine of the contact angle over time) obtained from a great number of experiments on different alloys were fitted with $n = 0.5$ and $n = 1$. An example for a Fe–0.5Mn alloy specimen is shown in Fig. 5, which has been fitted with the exponent values of $n = 0.5$ and $n = 1$, respectively. It can be remarkably visualized and concluded that the Avrami exponent, $n = 0.5$ (green curve) yields the best fit of the measured contact angle curve. Similar results were obtained for all other cases.

Figure 6 visualize the Fe–Al interfacial layer formation as well as the process of overgrowing the oxides. The surface morphology of Fe–1.5Si alloy annealed at dew point −30°C is shown in Fig. 6a. It shows the presence of large oxide islands (pale gray) on the surface and also sites where free iron is present together with a coverage by tiny oxide islands (darker gray), i.e., the overall coverage by oxide is much higher than the area covered by the light gray color would suggest. It is quite obvious that this alloy shows a high oxide coverage due to its high Si content. On this surface a zinc drop was placed and after 1-s reaction time the liquid Zn was removed by fast spinning, and then the alloy/Zn interface (i.e., Fe–Al interfacial layer) has been characterized by SEM (Fig. 6b). This clearly demonstrates the initial stages of Fe–Al interfacial layer formation at the metal/oxide boundary. In a second experiment, on an equivalently prepared Fe–1.5Si surface the drop was allowed for 3 s (reaction time) to stay on the surface of Fe–1.5Si alloy. Then again the residual liquid Zn was removed by fast spinning. The resulting morphology of the formed Fe–Al interfacial layer is shown in Fig. 6c. This is clearly showing the overgrowth of the oxide islands by the interfacial layer within 3 s of reaction time. The kinetic factor '*k*' (from the fit) and the experimental observation strongly correlate, pin-pointing that the surface coverage of oxide, their distribution, size, and surface chemistry play an important role in the reactive wetting.

The obtained results are evidencing that the spinning-off method is an excellent way to access the interface. Here, the reaction layer is revealed in its original state without any alteration by chemical etching as it is the case in the standard procedure where the zinc layer is removed by acidic attack. Moreover, as the results presented here clearly show, the experimental setup is well suited for revealing growth processes with high temporal resolution.

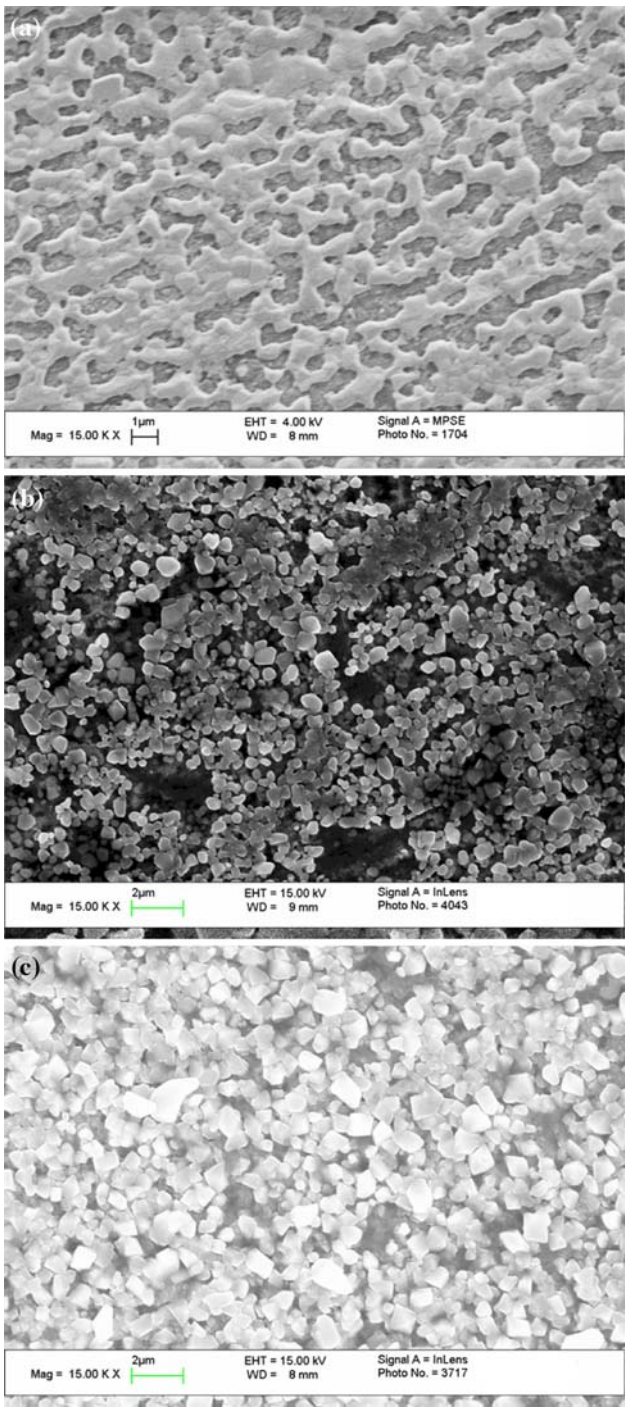

Fig. 6 **a** SEM image of the oxide coverage on a Fe–1.5Si alloy specimen annealed at dew point −30 °C, **b**, **c** are snapshots of the Fe–Al interfacial layer formation obtained by spinning-off the liquid zinc after 1 and 3 s, respectively

Conclusions

1. Hot Melt Rotator (HoMeR)—the novel setup, allows to study successively high temperature reactive wetting process. This setup basically combines the advantages of high temperature treatment under controlled atmosphere, contact angle recording, and easy surface analytical access to the reaction zone without further chemical treatment or even exposition to air.
2. The systematic investigation on the Fe–Si and Fe–Mn model alloys shed light on the understanding of reaction kinetics during hot-dip galvanizing process. The main result is that the Cassie equation combined with Avrami growth law is a good approximation for the wetting kinetics and also for the growth mechanism of the reaction layer. We also show that reactive wetting dynamics depend not only on the overall oxide coverage of the surface but also on the size of the oxide islands.

Acknowledgements This research was supported by the Research Program of the Research Fund for Coal and Steel, under contract RFS-CR-04021.

References

1. Eustathopoulos N, Nicholas MG, Drevet B (1999) Wettability at high temperatures. Pergamon, New York
2. Sobczak N, Singh M, Asthana R (2005) Curr Opin Solid State Mater Sci 9:149
3. Wang H, Wang F, Gao F, Ma X, Qian Y (2007) J Alloys Compd 433:302
4. Contreras A, Leon CA, Drew RAL, Bedolla E (2003) Scr Mater 48:1625
5. Marder AR (2000) Prog Mater Sci 45:191
6. Frenznick F, Stratmann M, Rohwerder M (2004) Galvatech Proc 411
7. Swaminathan S, Koll T, Pohl M, Wieck AD, Spiegel M (2008) Steel Res Int 79:66
8. Frenznick F, Stratmann M, Rohwerder M (2008) Rev Sci Instr 79:043901
9. Final Report: A mechanistic study of wetting and dewetting during hot dip galvanizing of high strength steels, Contract No. 7210-PR322, European Coal and Steel community (2005)
10. Grabke HJ, Leroy V, Viefhaus H (1995) ISIJ Int 35:95
11. Swaminathan S, Spiegel M (2008) Surf Interface Anal 40:268
12. Bordignon L, Crahay J (2001) Galvatech Proc 573
13. Mcdevitt Y, Moromoto M (1997) Meshii ISIJ Int 37:776
14. Baril E, Lesperance G (1999) Metall Mater Trans A 30A:681
15. Giorgi ML, Guillot JB (2005) J Mater Sci 40:2263. doi:10.1007/s10853-005-1944-5
16. Mandal GK, Balasubramaniam R, Mehrotra SP (2009) Metall Mater Trans A 40A:637
17. Webb EB III, Hoyt JJ, Grest GS, Heine DR (2005) J Mater Sci 40:2281. doi:10.1007/s10853-005-1946-3
18. Avraham S, Kaplan WD (2005) J Mater Sci 40:1093. doi:10.1007/s10853-005-6922-4
19. Protsenko P, Terlain A, Traskine V, Eustathopoulos N (2001) Scripta Mater 45:1439
20. Cassie ABD (1948) Discuss Faraday Soc 3:11
21. Avrami M (1941) J Chem Phys 9:177